

Spatial Forecasts of Maximum Hail Size Using Prognostic Model Soundings and HAILCAST

JULIAN C. BRIMELOW AND GERHARD W. REUTER

Department of Earth and Atmospheric Sciences, University of Alberta, Edmonton, Alberta, Canada

RON GOODSON

Prairie and Northern Region, Meteorological Service of Canada, Edmonton, Alberta, Canada

TERRENCE W. KRAUSS

Weather Modification Inc., Fargo, North Dakota

(Manuscript received 19 January 2005, in final form 5 October 2005)

ABSTRACT

Forecasting the occurrence of hail and the maximum hail size is a challenging problem. This paper investigates the feasibility of producing maps of the forecast maximum hail size over the Canadian prairies using 12-h prognostic soundings from an operational NWP model as input for a numerical hail growth model. Specifically, the Global Environmental Multiscale model run by the Canadian Meteorological Center is used to provide the initial data for the HAILCAST model on a $0.5^\circ \times 0.5^\circ$ grid. Maps depicting maximum hail size for the Canadian prairies are generated for 0000 UTC for each day from 1 June to 31 August 2000. The forecast hail-size maps are compared with radar-derived vertically integrated liquid data over southern Alberta and surface hail reports. Verification statistics suggest that the forecast technique is skillful at identifying the occurrence of a hail day versus no-hail day up to 12 h in advance. The technique is also skillful at predicting the main threat areas. The maximum diameter of the hailstones is generally forecast quite accurately when compared with surface observations. However, the technique displays limited skill when forecasting the distribution of hail on a small spatial scale.

1. Introduction

Hailstorms pose a serious economic problem for society. For example, losses exceeding \$300 million have become frequent in the United States since the 1990s (Changnon et al. 2000). Costly hailstorms have also been observed in Canada, with damages associated with a hailstorm that struck Calgary on 7 September 1991 estimated at \$400 million (Canadian) (Charlton et al. 1995). Severe weather algorithms, developed for weather radar, are routinely used to identify and now-cast the movement of hailstorms (Witt et al. 1998; Marzban and Witt 2001; Joe et al. 2004). However, lead

times of radar-based warnings are very short and the algorithms show limited skill at forecasting the actual hail size on the ground (Edwards and Thompson 1998). An alternative to radar-based hail algorithms is to use upper-air soundings to relate the maximum hail size on the ground to the estimated maximum updraft velocity (Foster and Bates 1956; Renick and Maxwell 1977; Moore and Pino 1990). Doswell et al. (1982), however, found significant shortcomings with buoyancy-based methods used to forecast hail size.

Brimelow et al. (2002b) proposed a new approach to forecast maximum hail size on the ground using HAILCAST, which is a one-dimensional steady-state cloud model combined with a time-dependent hail growth model. In that study, HAILCAST was run using observed proximity soundings. The predicted hail sizes were compared against reports of maximum hail size gathered from a high-density observation network within the Alberta Hail Project area. Brimelow et al.

Corresponding author address: Julian Charles Brimelow, Dept. of Earth and Atmospheric Sciences, University of Alberta, Edmonton, AB, T6G 2E3, Canada.
E-mail: brimelow@ualberta.ca

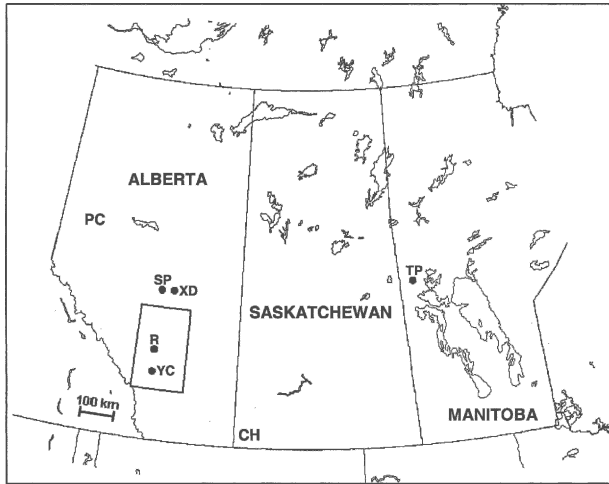


FIG. 1. Forecast domain of the GEM-HAILCAST hail forecasting technique for the summer of 2000. Here, SP and TP are the locations of the operational upper-air sounding sites at Stony Plain and The Pas, respectively. The city of Edmonton is located at XD, the city of Calgary at YC, the radar site at R, the Peace country near PC, and the Cypress Hills near CH. The large rectangle indicates the outline of the ASA.

(2002b) demonstrated that HAILCAST is skillful at forecasting the maximum expected hail size on the ground when initialized with representative proximity upper-air soundings and surface conditions. HAILCAST has subsequently been used in Argentina (Brimelow et al. 2002a), South Africa, and the United States (Jewell and Brimelow 2004).

The importance of using representative upper-air sounding data for predicting the maximum expected hail size cannot be overstated. Proximity soundings are usually identified by applying spatial and temporal constraints between the soundings and the observed storms (e.g., Brooks et al. 1994). However, in an operational setting, obtaining proximity soundings is complicated by the high spatial and temporal variability typically present in the prestorm environment and by the coarse spacing of upper-air networks. This is particularly relevant over the Canadian prairies where there are only two sounding sites (see Fig. 1): Stony Plain (53.53°N, 114.10°W) and The Pas (53.96°N, 101.10°W). These sites are almost 900 km apart and soundings are made only twice a day. Consequently, the observed soundings often are not representative of the antecedent thunderstorm conditions.

This study introduces an innovative hail forecasting technique that predicts where and when the largest hail is expected to fall with a lead time of up to 12 h. Our approach is based on using model soundings predicted by the Global Environmental Multiscale (GEM) model as input data for HAILCAST. The GEM model (Côté

et al. 1998) is the operational weather prediction model used by Environment Canada for issuing public and aviation forecasts. For the purpose of this study, GEM-forecasted soundings of temperature, humidity, and wind were generated on a 0.5° horizontal grid. These soundings provided the input for the cloud model.

The concept of using soundings predicted using NWP models for forecasting the intensity of convection has been explored before (Hart et al. 1998; Thompson 1998; Hamill and Church 2000; Thompson et al. 2003). Specifically, Hamill and Church (2000) and Thompson et al. (2003) found that the Rapid Update Cycle (RUC) model is generally capable of producing prognostic soundings, which can be used effectively to discriminate between environments that support thunderstorms of varying intensities. In this paper, we determine the feasibility of using prognostic GEM soundings to assist in forecasting the occurrence of hail over the Canadian prairies. We also examine the technique's skill in predicting the spatial distribution of hail and the maximum hail size.

For each day between 1 June and 31 August 2000, contour maps of the maximum forecast hail size on the ground (valid for 0000 UTC) were generated by running HAILCAST on a grid consisting of approximately 1400 GEM 12-h forecast soundings. The forecast hail maps were compared against radar reflectivity data and surface hail reports. The skill of the forecast technique was quantified using the probability of detection, false alarm ratio, and critical success index.

2. HAILCAST and the ensemble hail forecasting technique

HAILCAST consists of a steady-state cloud model linked to a hail growth model. The cloud model requires vertical profiles of ambient temperature, humidity, and wind. These data are used to compute vertical profiles of liquid water content, updraft velocity, and in-cloud temperature that are representative of the hail growth environment close to the updraft's near-adiabatic core. The time-dependent hail model then uses these data to simulate the growth of hail in the updraft. A drizzle-sized hail embryo is introduced at cloud base and then grows by either wet or dry growth. Allowance is made for melting of the hailstone as it descends below the in-cloud freezing level. During wet growth (melting), excess accreted water (meltwater) on the surface of the stone is shed. The current version of HAILCAST does not allow hailstones to fall through an unsaturated downdraft below cloud base. Consequently, the anomalously warm air below cloud base could increase the predicted amount of melting (espe-

cially for small hailstones). However, given that freezing levels typically observed over the study area (section 4a) are relatively low (3.5–4.0 km above sea level) and that we are primarily concerned with predicting severe hail, the potential increase in melting rates is not expected to significantly affect our results. Details of the HAILCAST model are provided in Brimelow et al. (2002b).

One of the challenges facing forecasters when predicting the initiation and strength of convection is the spatial distribution of moisture in the boundary layer. Low-level moisture and temperature fields are not homogeneous and variability can occur on scales that are much smaller than those of most observation networks. For example, Weckwerth (2000) noted the effects of small-scale moisture variability evident in horizontal convective rolls on thunderstorm initiation. This uncertainty complicates the already difficult task of predicting convective initiation.

Mueller et al. (1993) and Crook (1996) employed multidimensional cloud models to study the sensitivity of thunderstorm initiation and intensity to fluctuations of temperature and moisture in the boundary layer. Their experiments demonstrated that the modeled convection was sensitive to small changes in the surface input data. Specifically, Crook found that small variations in the surface temperature (1°C) and moisture (1 g kg^{-1}) could differentiate between no convection and intense convection. Similarly, model sensitivity experiments showed that model output from HAILCAST was sensitive to changes as small as 1°C in the surface temperature and dewpoint (Brimelow 1999).

To improve our ability to predict the evolution of the atmosphere, one can perform a number of model simulations (or ensemble members), each starting with slightly different initial conditions (Crook 1996). Brooks et al. (1992) suggested adopting a quasi-Monte Carlo, or probabilistic approach, when employing numerical cloud models to forecast convection. This approach involves varying the input data for the cloud model over a range of values expected in the area where convection is anticipated. Assuming that the range of initial conditions spans the domain of the expected error, the ensemble mean may provide a more skillful forecast than the majority of the individual forecasts. Adopting an ensemble approach has been found to mitigate the sensitivity of numerical weather prediction model forecasts to uncertainties in the input data (e.g., Stensrud et al. 2000).

HAILCAST is computationally efficient and is thus well suited for producing ensemble forecasts. In this study, the ensemble forecasts were prepared by adding perturbations of -1.0° , -0.5° , 0° , $+0.5^{\circ}$, and $+1.0^{\circ}\text{C}$ to

both the GEM forecast temperature and dewpoint at each surface grid point. HAILCAST was then run for each combination of the temperature and dewpoint, resulting in a total of 25 individual hail diameter forecasts. The ensemble diameter was determined by calculating the arithmetic mean of all 25 forecast hail diameters. The above ranges in temperature and dewpoint were selected to represent the surface temperature and moisture variations expected in the boundary layer on any given day. At this stage, we only vary the surface temperature and dewpoint, because sensitivity tests conducted by Brimelow (1999) showed that of all the parameters considered, small variations in the surface temperature and dewpoint overshadowed the changes in the modeled hail size achieved by varying other microphysical parameters in the hail model. The forecast profiles of temperature, dewpoint, and wind above the surface were assumed to remain unchanged.

In this study, no information concerning the uncertainty of the forecast (i.e., standard deviation) or probability of the forecast hail size exceeding critical thresholds is extracted from the ensembles. As an alternative approach to the Monte Carlo technique used here, one could conceivably create a group of ensemble members by running HAILCAST using prognostic soundings generated by the NWP ensemble at each grid point. This approach would take into account variations in the temperature, moisture, and wind profile throughout the atmospheric column. Alternatively, one could create an ensemble by varying some of the microphysical parameters or parameterization schemes used in the hail model. Based on the sensitivity experiments of Brimelow (1999) and Brimelow et al. (2002b), some parameters that could be considered for this purpose are the collection efficiency of ice, the ice density, and the initial embryo diameter.

3. Prognostic sounding data

Our study focused on three Canadian prairie provinces: Alberta, Saskatchewan, and Manitoba (Fig. 1). The forecast technique was evaluated for 92 days between 1 June and 31 August 2000. To capture the pre-storm environment on each day, we used prognostic upper-air soundings produced by the 1200 UTC run of the 24-km resolution GEM model. In this study, a total of 1403 Gridded Binary (GRIB) format soundings were generated for 0000 UTC at 0.5° intervals between 49° and 60°N and 120° and 90°W . The forecast pressure, height, temperature, dewpoint, and wind speed and direction were available at 14 vertical levels between the surface and 150 hPa. HAILCAST was run at each grid

point and the resulting field of hail diameters was then contoured to create spatial maps of the maximum expected hail size.

It is important to note that the forecast profiles of moisture and temperature in the low levels of the atmosphere can differ from those observed in nature due to shortcomings in the NWP models. For example, steep orography, model boundary layer parameterizations, data assimilation methods, and land use category schemes represent only a few of the complex factors that can have an important impact on NWP output (Hanna and Yang 2001; Case et al. 2002). The parameterization of convection in NWP models is another potential source of uncertainty in the forecast profiles (Grell et al. 1991; Grell 1993; Baldwin et al. 2002).

The purpose of convective parameterization (CP) schemes is to simulate the effects of the release of latent heat and the vertical transport of sensible heat and water vapor on the vertical profile of atmospheric temperature and moisture following the onset of convection. Specifically, CP schemes reduce the instability by rearranging the temperature and moisture distribution in a model grid column as determined by the net effects of latent heat release, cloud entrainment and detrainment, and evaporatively driven downdrafts.

Model prognostic soundings may contain inaccuracies on account of errors in the numerical data fields that specify the amount of instability prior to convection initiation, erroneous prediction of the timing and location of convection, and errors in the expected evolution of the convection (e.g., Grell 1993). In addition to the aforementioned errors, errors can also arise from modifications to the temperature and moisture profiles once the convection parameterization scheme is initiated. For example, the Betts–Miller–Janjić (BMJ) parameterization scheme (Betts 1986; Betts and Miller 1986; Janjić 1994) used in the National Centers for Environmental Prediction Eta Model has been found to remove small-scale vertical features, such as capping lids or stable layers, once convection is initiated (Baldwin et al. 2002). In other words, using certain CP schemes can modify prognostic soundings, at grid points where convection has been triggered, resulting in forecast profiles that are not representative of the pre-storm environment.

The version of the GEM used in this study employed the Fritsch–Chappell scheme (Fritsch and Chappell 1980) to simulate convection. In the Fritsch–Chappell scheme, numerical model data fields are used to place limits on the available buoyancy, while an entraining cloud model is used to estimate the vertical mass fluxes that are required to satisfy the limits (Fritsch and Chappell 1980). When convection is triggered at a model grid

point, the scheme assumes that the convection removes the convective available potential energy within a time interval determined by the time convection is active in a grid element. The FC scheme is subject to similar uncertainties and limitations as observed in other CP schemes. For example, the limits imposed on time convection (30–60 min) can cause the model to maintain convection for too long (or too short) at a grid point when the mean flow in the cloud layer is very strong (or very weak) (Fritsch and Kain 1993).

4. Verification data

a. Surface hail report database

In total, 533 reports of hail were collected for the period between 1 June and 31 August 2000 for the purpose of verifying the accuracy of the HAILCAST hail size forecasts. Using surface hail reports has inherent problems, including uncertainty regarding the accuracy of the time and location the hail occurred, as well as the accuracy of the hail-size measurements (Lenning et al. 1998). The latitude, longitude, and time of a given hailstorm were only available for the U.S. Storm Prediction Center (SPC) and Meteorological Service of Canada (MSC) reports, which accounted for less than a third of all the reports collected. SPC reports of severe hail made within 0.5° latitude (~ 55 km) of the U.S.–Canada border were included in the database. For the remaining reports, the latitude and longitude of the town where the hail was reported were used to specify the location of the hail events. The SPC reports were obtained from the preliminary severe weather log, but were corroborated using the final storm log. Lightning data were used to ensure that convection occurred in the immediate vicinity of the hail reports and to determine whether the hail fell between 2000 and 0500 UTC. This time frame was selected to increase the likelihood that the 0000 UTC GEM forecast soundings would be representative of the convective environment.

The majority of the surface hail reports (332 or 62%) were obtained from the Alberta Agriculture Financial Services Corporation, with 153 (29%) coming from the MSC severe weather database, 28 (5%) from Weather Modification Inc., and 20 (4%) from the SPC severe weather database. Of the 533 hail reports in the database, 425 (almost 80%) of the hail reports were from Alberta, compared to 77 (14%) from Saskatchewan and 31 (6%) from Manitoba.

Table 1 summarizes the hail reports by hail-size category. If, on a given day, more than one hail report was received from the same location, the largest size was used. A hail day was classified as severe when the reported (or forecast) hail diameter was 2.0 cm or larger.

TABLE 1. Summary of hail categories and numbers of reports per size category, received between 1 Jun and 31 Aug 2000.

Diameter range (cm)	Category	Representative diameter (cm)	No. of reports over prairies	No. of reports over ASA
0.5–1.2	Pea	0.75	119	44
1.3–1.9	Grape	1.5	149	59
2.0–3.2	Walnut	2.5	131	25
3.3–5.2	Golfball	4.0	118	20
≥5.3	>golfball	6.0	16	3

According to surface reports, 61 (66%) of the 92 days in the dataset were identified as hail days. Of these, 44 (72%) were classified as severe hail days. There were 268 reports of nonsevere hail and 265 reports of severe hail. Reports of grape-sized hail were the most frequent (28% of all reports), followed by walnut-sized hail (25%). The number of reports of pea-sized hail and golfball-sized hail were almost the same (22%). Only 3% of the reports were for larger than golfball-sized hail.

Figure 2a shows all of the locations where hail was reported between 1 June and 31 August 2000. The high concentration of hail reports over south-central Alberta is evident. The reports also reflect the presence of the main highway between Edmonton and Calgary. Very few reports of hail were received north of 55°N. This is probably, in part, a result of the low population density, which is less than 1 km^{-2} over the majority of the Canadian prairie provinces and only exceeds 10 km^{-2} over a few localized areas.

Figure 2b depicts the spatial distribution of hail days observed in 1° latitude \times 1° longitude grid boxes. As expected, the spatial distribution of the hail days shown in Fig. 2b is very similar to that of the hail reports shown in Fig. 2a. The highest frequency of observed hail days occurred in the Edmonton–Calgary corridor, with 19 hail days reported over the foothills northwest of Calgary. A local maximum is also evident east of the Cypress Hills in southwestern Saskatchewan. The number of reported hail days decreases rapidly in regions located outside south-central Alberta. A very similar pattern is evident for the distribution of severe hail reports (not shown), with the most severe hail reports being received over south-central and central Alberta, where approximately five severe hail days were reported. Outside Alberta, the number of reported severe hail days decreased rapidly.

Because of the low population density over the majority of the Canadian prairies, many hailstorms go undetected. Thus, surface hail reports alone are not suitable for verifying high spatial resolution forecast hail

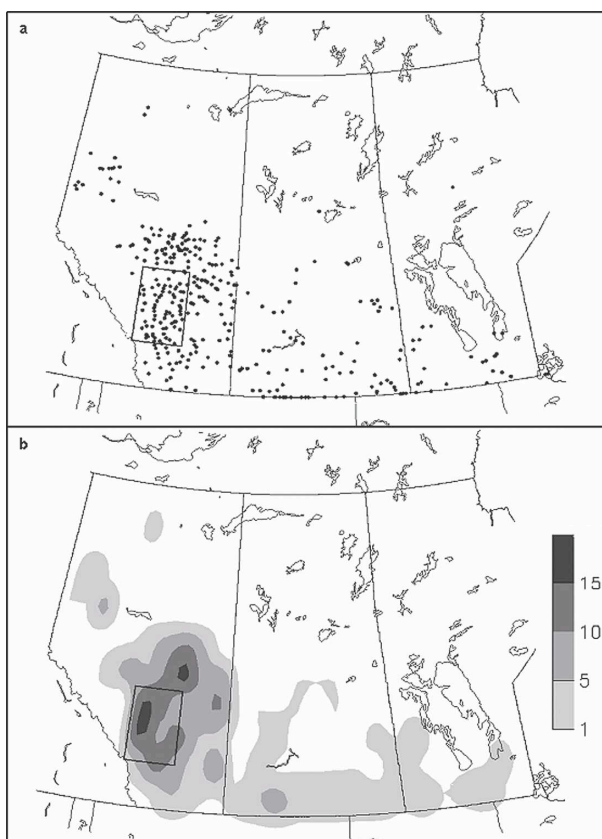


FIG. 2. Hail reports for the period 1 Jun–31 Aug 2000. Shown are (a) locations of hail reports and (b) grayscale contour map depicting the number of hail days observed within 1° lat \times 1° lon boxes.

maps. To include as many hail events as possible we focused our verification of the forecasts over a $2.5^\circ \times 2.5^\circ$ box (175 km east–west by 275 km north–south) over south-central Alberta (Fig. 1). This Alberta study area (ASA) encompasses the climatologically preferred region for hailstorms (Etkin and Brun 1999). Further, the summer of 2000 was an active season for convection over the ASA. In addition, the area of the ASA (48 000 km^2) is similar in area to the typical watch area issued by the U.S. Storm Prediction Center (40 000–50 000 km^2) and Canada's Prairie Storm Prediction Center.

b. Radar reflectivity data

To avoid the problems associated with relying on a sparse surface observation network to report hail, we used radar data to infer the presence of hailstorms. The advantage of weather radar is that, by virtue of its continuous space and time coverage, it detects all precipitating cells within its viewing area. Radar reflectivity data for the period 1 June–31 August 2000 were col-

lected by a C-band radar located at the Olds-Didsbury airport (51.71°N, 114.11°W, elevation 1024 m) in southern Alberta (Fig. 1). Volume scans were performed at 5-min intervals throughout the summer. The radar transmits at a peak power of 250 kW, has a beamwidth of 1.65°, and a range gate size of 900 m. Most of the ASA was located within 150 km of the radar site, which would minimize sampling errors. Radar data were displayed using the Thunderstorm Identification, Tracking, Analysis, and Nowcasting cell tracking system (Dixon and Wiener 1993). The radar performance parameters were checked weekly and a complete calibration was performed each month during the summer.

Lenning et al. (1998) found that the use of radar-derived vertically integrated liquid (VIL) water content was promising for indicating the presence of hail in thunderstorms near Tallahassee, Florida. Specifically, they indicated that selecting VIL thresholds can be useful for distinguishing between significant and marginal hail events, and between marginal and nonevents. Brimelow et al. (2004) also found VIL data useful for identifying observed hailfall over central Alberta. Specifically, comparisons with surface hail reports indicated that a VIL threshold of 25–30 kg m^{-2} was effective at correctly identifying those storms associated with reports of severe hail over central Alberta. Comparisons of VIL measurements with hail reports over Alberta suggest that an appropriate lower VIL threshold for hail is 10 kg m^{-2} . Likewise, Kitzmiller et al. (1995) noted that VIL values in organized convective cells usually exceeded 10 kg m^{-2} .

Using the guidelines of Brimelow et al. (2004), a day in the ASA was classified as a probable hail day if the VIL at one or more pixels ($\sim 1 \text{ km}^2$) was larger than or equal to 10 kg m^{-2} . If the VIL exceeded 25 kg m^{-2} at two or more contiguous pixels ($\sim 3 \text{ km}^2$), then the day was classified as a severe hail day. The maximum VIL maps were created by recording the maximum VIL observed at each pixel in the radar's domain. Figure 3 shows an example of a maximum VIL map (valid for 4 July 2000) that was used to verify the hail forecasts and hail reports. The locations where hail was reported are also indicated on the map. The location and severity of the 10 surface hail reports corresponded well with the radar-derived VIL data. However, there were several locations without surface hail reports, yet the VIL values were the same or higher than at those locations where hail was reported. Specifically, there were at least 15 locations over the ASA where the VIL data suggested that hail was likely present but no surface reports of hail were received. This day is a typical example of cases when using surface hail reports alone

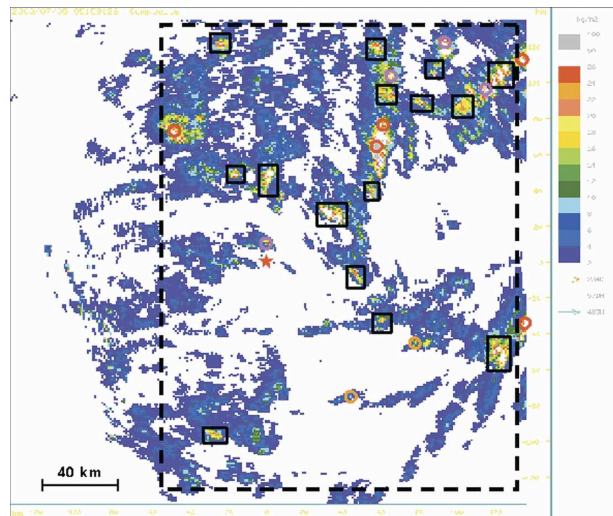


FIG. 3. Maximum VIL map for the ASA (large dashed rectangle) on 4 Jul 2000. Orange circles represent locations where pea-sized hail was reported, pink circles the locations where grape-sized hail was reported, and red circles locations where walnut-sized hail or larger was reported. The red star indicates the location of the Olds-Didsbury radar. Black rectangles represent locations where the VIL field indicated the presence of hail but no hail was reported.

would have underestimated the occurrence of hail in sparsely populated areas.

The daily maximum VIL maps included the locations of observed hail reports with few exceptions. In fact, there were only three occasions (of 151 hail reports) when reports of hail were received over the ASA, but the VIL maps did not indicate the presence of hail. For one event, attenuation of the radar signal by a severe storm located between the radar and the report probably was responsible for the radar underestimating the strength of the distant hailstorm. The two remaining reports were both located more than 120 km from the radar, where VIL values were $\sim 9 \text{ kg m}^{-2}$, which is just below the 10 kg m^{-2} threshold used for hail.

Radar indicated that hail was likely present on 9 days when no reports of hail were received over the ASA. Similarly, radar indicated the potential for severe hail over the ASA on 4 days when no hail reports were received. Radar also indicated severe hail on 11 days when reports of nonsevere hail were received. On 9 of these days, grape-sized hail was reported, while on the remaining 2 days pea-sized hail was reported. The absence of severe hail reports on certain days could be because the observers failed to measure the largest hail size, or because severe hail fell over a sparsely populated area.

Studies investigating the utility of VIL as an indicator of severe hail have shown that severe VIL thresholds

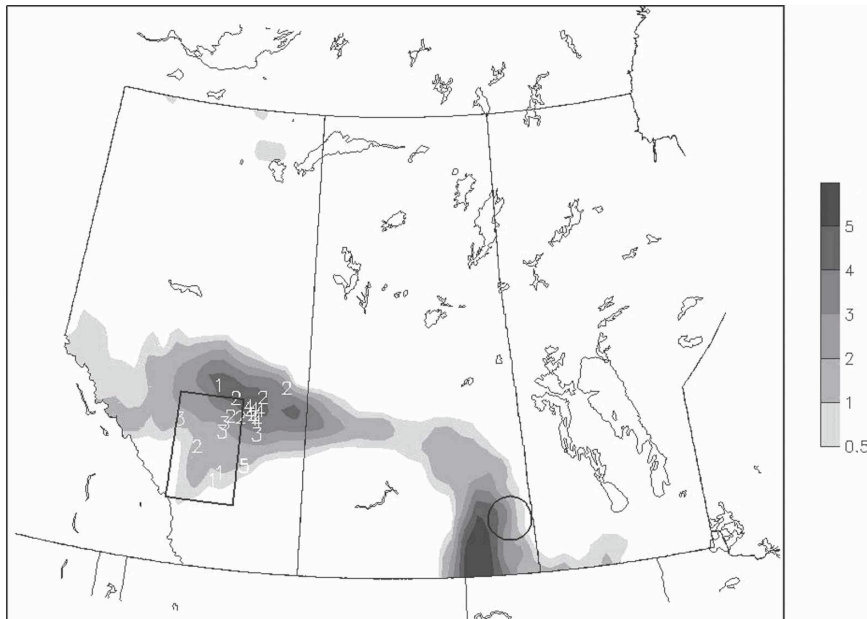


FIG. 4. Hail forecast map generated using prognostic GEM soundings and HAILCAST for 4 Jul 2000. Forecasted hail diameters are contoured in cm. The large rectangle encloses the ASA and the circle over southeastern Saskatchewan indicates where weather radar observed several strong thunderstorms. Surface hail reports are indicated by numbers, with a 1 representing pea-sized hail (0.5–1.2 cm); a 2, grape-sized hail (1.3–1.9 cm); a 3, walnut-sized hail (2.0–3.2 cm); a 4, golfball-sized hail (3.3–5.2 cm); and a 5, greater than golfball-sized hail (>5.2 cm).

display a strong regional dependence (Wagenmaker 1992; Kitzmiller et al. 1995; Edwards and Thompson 1998). Consequently, Paxton and Shepherd (1993) proposed an algorithm to calculate an appropriate VIL threshold for severe hail that is dependent on the air-mass characteristics. This threshold is referred to as the VIL of the day or VOD. On all days when the observed VIL was larger than or equal to 26 kg m^{-2} , the maximum VIL observed over the ASA exceeded the VOD calculated from the 0000 UTC Stony Plain sounding. It is thus unlikely that a day was incorrectly classified as a severe hail day. In addition, it is unlikely that the threshold of 26 kg m^{-2} to identify severe hail was too high, as none of the 48 severe hail reports over the ASA were associated with maximum VIL values of less than 26 kg m^{-2} .

5. Comparison of a HAILCAST map and observations for 4 July 2004

Figure 4 shows a map of the forecast hail size valid for 0000 UTC 5 July 2004. The grayscale is labeled in centimeters for the largest expected hail diameter. HAILCAST was initialized using the prognostic GEM soundings from the 1200 UTC model run. On this day, several severe thunderstorms produced golfball-sized hail over east-central Alberta. The location and size of the hail reports suggested that the HAILCAST guid-

ance was good, with eight of the nine severe hail reports located in close proximity (<50 km) of the forecast 2-cm hail contour. Also, the maximum forecast hail diameter of 4–5 cm agreed well with the reports of golfball-sized hail. The forecast indicated that the potential for severe hail decreased as one moved southwestward from the region of large hail forecast over central Alberta. This tendency was supported by surface reports and radar data (Fig. 3), with no severe hail being reported or indicated over the southern ASA.

The model also indicated that the potential existed for large hail over far southeastern Saskatchewan. Although no reports of severe hail were received from this area, weather radar identified several strong thunderstorms in the area enclosed by the circle in Fig. 4 between 0000 and 0300 UTC. The maximum reflectivity observed in these storms was between 50 and 55 dBZ, which suggests that hail may have been present at the surface (Barge 1974; Changnon 1992).

6. Validation of HAILCAST

a. Forecasting of hail day or nonhail day within the ASA

In this section we quantify the forecast skill of HAILCAST to predict the occurrence of hail anywhere

within the ASA. In other words, we test whether HAILCAST can predict accurately a hail day versus a nonhail day. Given the problems associated with the surface report database discussed in section 4, hail forecasts were verified using maximum VIL maps from the Olds-Didsbury radar.

Smith and Yau (1993) confirmed earlier studies that suggested that hailstorms typically develop over central Alberta when there is a "favorable" synoptic-scale height pattern at 500 mb. Specifically, Smith and Yau's study showed that hailstorm activity is usually associated with a 500-mb trough over or upstream of Alberta. Based on Smith and Yau's findings, we examined the 1200 and 0000 UTC 500-hPa upper-air analysis charts for each day to classify the upper airflow over and upstream of the ASA (a region bounded by 45°–55°N and 110°–125°W). Particular attention was paid to the direction of the flow at 500 hPa and changes in 500-hPa heights between 1200 and 0000 UTC. Each of the 92 days was then categorized as being either favorable for hailstorms (i.e., 500-mb trough or perturbation) or unfavorable for hailstorms (i.e., 500-mb ridge).

Careful analysis of upper-air charts revealed that the upper airflow favored the formation of hailstorms on 44 days during the study period. Comparison of the upper-air charts and maximum VIL maps for the summer of 2000 suggests that there was a positive correlation between hail activity over the ASA and the presence of an upper-air trough. In particular, of the 45 hail days observed by radar over the ASA, 71% were associated with an upper-air trough. By comparison, hail was observed by radar on almost 73% of the days when an upper-air trough was present. Radar detected severe hailswaths that were more than 50 km in length on 11 days, and on 8 (73%) of these days an upper-air trough was present. In contrast, only 10% of the hail days and 15% of the severe hail days were observed when the flow was deemed unfavorable for hailstorms.

Before discussing the performance statistics, it must be kept in mind that HAILCAST was not designed to explicitly predict the initiation of convection. Rather, the model provides an estimate of the maximum expected hail size given that convection is triggered. Notwithstanding this caveat, the model can still potentially improve lead times of warnings because forecasters can be proactive when issuing warnings on those occasions when storms that are moving into an area where the potential for large and damaging hail exists as indicated by HAILCAST.

The skill of HAILCAST to predict the occurrence of a hail day or a nonhail day within the ASA was quantified using the probability of detection (POD), the false alarm ratio (FAR), the critical success index

TABLE 2. Skill scores calculated for predicting the occurrence of hail or severe hail within the ASA for the summer of 2000. Values under column T were calculated only using the model guidance on days when there was an upper-air trough upwind or over the ASA; scores under column A are the skill scores calculated for all days in the dataset.

	All hail days (%)		Severe hail days (%)	
	T	A	T	A
POD	90	93	75	79
FAR	26	45	32	45
CSI	68	53	56	48
HSS	16	22	46	45

(CSI), and the Heidke skill score (HSS). These skill scores are commonly used (e.g., Marzban and Stumpf 1998). The disadvantage of using this approach to verify the forecast skill is that the model could forecast hail up to 250 km from the location where hail was observed and still score a hit.

Table 2 shows the performance statistics calculated for predicting hail anywhere over the ASA when the upper-air circulation was favorable for hailstorms. The hail forecasting technique scored a POD of 0.90, an FAR of 0.26, a CSI of 0.68, and an HSS of 0.16. Note that, by adopting this approach, the POD reflects the number of hits on days when the upper-air circulation pattern favored organized storms and, consequently, hail days observed when the flow was unfavorable (13) would have been missed. The POD for forecasts of severe hail when an upper-air trough was present was significantly lower than that calculated for all hail days (0.75 versus 0.90), while the FAR was somewhat higher (0.32 versus 0.26). Consequently, the overall forecast skill for severe hail days was lower than for all hail days, with a CSI of 0.56. In contrast, the HSS for severe hail days was markedly higher (0.46 versus 0.16). The superior performance suggested by the HSS could be attributed to the fact that the CSI does not give credit for null forecasts, and almost 40% of the forecasts for severe hail were null forecasts, compared to only 7% of those forecasts for hail of any size. This suggests a tendency for the hail forecasting technique to overpredict the occurrence of hail on trough days.

We also calculated the skill scores using all days (i.e., both synoptically favorable and unfavorable 500-mb flow patterns). This resulted in the FAR increasing between 13% and 19%, with only a slight increase (about 3%) in the POD. This was to be expected given that 71% of all of the false alarms for hail were observed on days when the upper-air circulation was classified as unfavorable for hailstorms. Accordingly, the overall performance of the forecast technique (as quantified by

the CSI) was reduced between 8% and 15% when the forecasts for all days were considered. By comparison, the HSS for forecasts on all hail days increased by 6%. This increase in the HSS could be ascribed to the fact that about 15% of the forecasts made for all days in the dataset were null forecasts, compared to only 7% of the days when an upper-air trough was present. The HSS of 0.46 obtained for the severe hail forecasts was almost the same as that achieved when forecasts were only considered for trough days.

b. Forecasting the spatial distribution of hail within the ASA

The second, more stringent, verification method was similar to that developed by Weiss et al. (1980) for the purpose of verifying SPC outlooks and watches. Weiss et al. addressed the problem of evaluating the skill of large spatial forecasts (approximately 100 000 km²) using a low-density event verification dataset. They noted that, while the POD is not affected by the size of the verification area, the FAR tends to increase as the verification area increases. For example, they found that FARs of 0.9 were typically achieved when they evaluated severe weather watches having an average area of about 100 000 km². The reason for this is that although the atmosphere can be unstable over very large areas, convection typically occurs only over a fraction of that area—this is especially true for severe convection. To try and address this problem, Weiss et al. recommended equating each surface report of severe weather with a much larger area. Their rationale for adopting this approach is that SPC forecasters do not anticipate severe weather over the entire severe weather watch area. Likewise, if HAILCAST predicts hail over the entire ASA, we do not expect that hailstorms will cover the entire area. The verification methodology developed by Weiss et al. was also designed to take into account the spatial distribution of the surface reports so as to mitigate biases that event clustering may have introduced into the verification statistics. We adopted the method of Weiss et al. as follows.

1) The ASA was divided into 25 blocks. Each block measured to be 0.5° by 0.5° (~1900 km²). This is similar to the area of the manually digitized radar blocks (~1700 km²) used by Weiss et al. A block was only counted as a forecast hail (severe hail) block if hail (severe hail) was forecast to cover at least 50% of the block. If the maximum VIL maps indicated hail (severe hail) in a given block, then that block was tagged as a hail (severe hail) block. Figure 5 illustrates how the verification technique was applied over the ASA. Blocks in which hail was

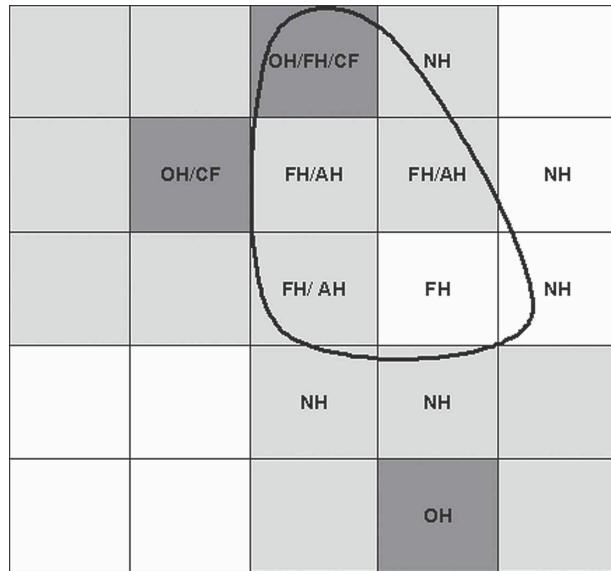


FIG. 5. Schematic illustrating the verification technique (see section 6b for details).

reported (OH) are shaded dark gray. The area forecast to receive hail is enclosed by the heavy line. Blocks labeled FH (NH) were forecast to receive more (less) than 50% hail coverage.

- 2) Errors in the location of certain fields forecast by GEM (such as CAPE) could be attributed to timing errors. For example, the model may have predicted that an area favorable for severe convection at 0000 UTC was farther west (or east) of the area where the hailstorms actually developed at that time. Alternatively, assuming that GEM correctly forecast the area at threat of hailstorms at 0000 UTC, it is possible that some of the hail fell a few hours before (or after) 0000 UTC when the area favorable for deep convection was located some distance upwind (or downwind). Thus, to allow for timing errors in the forecast fields, and to compensate for the fact that convection typically covers small areas and the uncertainty in the location of hail reports, an observed hail block was deemed to also verify the forecast occurrence of hail in all the blocks bordering that block (see blocks shaded light gray in Fig. 5). On most occasions, this criterion required the hail forecast to be within 35–55 km of the observed hailswath; the farthest distance that the forecast hail contour could be from a hailswath and still be considered a hit was approximately 90 km. The exact distance depended on the location of the hailswath relative to the forecast hail contour.
- 3) Observed hail blocks (along hailswaths) that occurred within one block of the forecast hail (FH)

block(s) were deemed to be correctly forecast (CF). The POD was calculated by dividing the sum of CF blocks by the sum of observed hail (OH) blocks. The daily counts of CF and OH were then summed between 1 June and 31 August 2000 to calculate the POD over the ASA for the entire summer:

$$\text{POD} = \sum \text{CF} / \sum \text{OH}. \quad (1)$$

Referring to Fig. 5, the two hail events observed in the northwest were CF because hail was forecast within one block of both OH blocks. The hail block in the southeast does not count toward \sum CF because there were no forecast hail blocks adjacent to it.

- 4) The first step in calculating the FAR was to calculate the “good percentage area” (Weiss et al. 1980). This parameter represents the fraction of the area forecast to receive hail that was actually affected by hail. To this end, the sum of all those *forecast* hail blocks that bordered the observed hail blocks was calculated (AH). In Fig. 5, blocks labeled AH are not counted as false alarms even though no hail was observed in those blocks. The good percentage area was then calculated by dividing the sum of AH by the sum of all of the blocks forecast to receive hail (FH). The concept of the good percentage area is still used operationally by the SPC when verifying watches or outlooks for severe weather. The FAR was calculated using

$$\text{FAR} = 1 - \left(\sum \text{AH} / \sum \text{FH} \right). \quad (2)$$

- 5) Finally, the overall skill of the forecasts was calculated using the CSI. The CSI varies between 0 for no skill and +1 for perfect skill. The CSI was calculated using

$$\text{CSI} = [(\text{POD})^{-1} + (1 - \text{FAR})^{-1} - 1]^{-1}. \quad (3)$$

As mentioned previously, this verification technique applies spatial criteria on the forecast hail maps. In particular, the model is penalized if hail is forecast over a large area and hail occurred only over an isolated area.

Considering model forecasts only on days when the upper-air circulation was favorable, Table 3 shows that the POD over the ASA for all hail blocks was 0.84, with an FAR of 0.41 and a CSI of 0.54. An FAR of 0.41 indicates that 59% of the blocks forecast to receive hail were within one block of the observed hailswaths. On the severe hail days, the POD was significantly lower at 0.60, with an FAR of 0.53; the lower POD was primarily responsible for the inferior CSI of 0.36. A possible explanation for the higher FAR for the forecasts on se-

TABLE 3. Same as in Table 2 except skill scores are calculated for predicting the occurrence and location of hail–severe hail over the ASA for the summer of 2000.

	All hail days (%)		Severe hail days (%)	
	T	A	T	A
POD	84	87	60	66
FAR	41	54	53	57
CSI	54	43	36	35

vere hail days is that, on average, the severe hailswaths (observed by radar) covered a small area of the ASA (17%), while the model forecast severe hail over a relatively large area (29%). The small areal coverage of severe hailswaths would also make it more difficult to correctly forecast their position, which would in turn reduce the likelihood of a hit. A negative bias of almost 1 cm when predicting severe hail (see section 6c) could also, in part, have contributed to a lower POD.

Table 3 indicates that including forecasts for all days in the calculation of verification statistics increased the FAR, while only resulting in a small increase in the POD. This was especially noticeable for the forecasts on all days, with the FAR increasing by 13% and the POD increasing by only 3%. In contrast, verifying forecasts of severe hail on all days resulted in only a slight decrease in the skill of the forecasts, with the 4% increase in the FAR offset by a 6% increase in the POD.

In summary, over the ASA, HAILCAST has greater skill at forecasting the occurrence of a hail day or a no-hail day than at predicting the spatial distribution of the hailstorms. Generally, applying the spatial and areal constraints on the hail forecasts lowered the forecast skill by reducing the number of hits and by increasing the number of false alarms. Caution must be exercised in directly comparing the performance statistics calculated using the two verification techniques, as the methodologies used to calculate the skill scores are different.

c. Forecasting the maximum hail diameter

The forecast hail diameters were obtained by running HAILCAST using prognostic GRIB soundings interpolated to the latitude and longitude of the hail reports. To allow for uncertainty in the time and location of the hail reports, tight gradients in the forecast hail maps, and timing errors in the GEM model, HAILCAST was also run using a prognostic sounding valid for 2100 UTC. The 2100 UTC soundings were constructed by linearly interpolating the forecast data (at each level) valid for 1800 and 0000 UTC. The largest of the 2100 and 0000 UTC forecast hail sizes was then used to cal-

TABLE 4. Summary of performance statistics calculated to quantify the accuracy of the hail-size category forecasts for hail/severe hail days over the ASA and for all hail reports on the Canadian prairies in 2000.

	ASA		All reports	
	All hail	Severe	All hail	Severe
Hail-size category (%)				
Correct	30	39	29	33
Within one	76	76	73	71
One too small	23	33	22	27
Two or more too small	8	24	12	26
One too large	23	4	22	11
Two or more too large	16	0	15	4
Hail-size error (cm)				
Mean error	0.3	-0.9	0.1	-0.7
Mean absolute error	1.2	1.2	1.3	1.5

culate the forecast hail-size category. Errors and hail-size category statistics were only calculated for those reports when the hail model forecast hail of at least 5 mm in diameter. In other words, we wished to establish how accurate the forecast hail sizes were, given the condition that a forecaster was expecting hail. By applying this criterion, 423 (almost 80%) of the 533 surface hail reports in the dataset were used to verify the accuracy of the forecast hail sizes. The mean errors and absolute errors were calculated by subtracting the observed hail diameter from the forecast hail diameter on the ground. Hail reports were allocated a representative diameter (according to Table 1) if no specific diameter measurement was provided; otherwise, the reported diameter was used to calculate the hail-size error.

Table 4 shows that, over the ASA, 30% of the categorical hail-size forecasts were correct and 76% were correct to within one size category. Very few of the forecasts were off by two or more categories. About 80% of the hail-size forecasts were within 2 cm of the observed diameters, while only approximately 5% of the errors were greater than 3 cm. The mean absolute error for the hail-size forecasts was 1.2 cm, with a positive bias of 0.3 cm. The accuracy of the hail-size forecasts for all of the prairies was comparable, albeit slightly less so.

The hail-size forecasts for severe hail days were comparable with those for all hail days, with 76% correct to within one hail-size category. Almost 40% of the hail category forecasts were correct. There was a tendency for the forecasts to underestimate the hail category for severe events, with 57% of the forecasts one or more categories too small. About 25% of the forecasts were two or more categories too small. This tendency to underestimate the hail-size category for severe events is

reflected in the negative bias of -0.9 cm. Jewell and Brimelow (2004) noted a similar negative bias in hail-size forecasts produced using HAILCAST and proximity soundings for 392 severe hail events over the contiguous United States between 1997 and 2002.

Forecasts of hail size for severe events across all three provinces were slightly less accurate. The close correspondence between the hail-size category and error statistics for hail forecasts for events over the ASA and those for all three prairie provinces suggests that the hail forecasts did not display a marked regional bias.

7. Accumulated hail maps

We also wished to determine whether the frequency and distribution of hail during the summer of 2000, as forecast by the GEM soundings and HAILCAST, were consistent with the hail climatology over the Canadian prairies. Ideally, the hail forecasting technique would predict the highest frequency of hail in areas that typically experience a high incidence of hail and would predict the lowest frequency of hail in areas where hailstorm activity is typically low. To this end, maps of the forecast hail frequency were generated by summing the number of hail days forecast by HAILCAST at each GRIB sounding location between 1 June and 31 August. The total number of days when severe hail was forecast at each grid point was also calculated. These data were then contoured to produce Fig. 6.

Figure 6a shows that the highest frequency of hail days (approximately 50) was forecast to occur in a band running parallel to the Continental Divide over southwestern Alberta. The frequency of hail was forecast to decrease steadily east of the foothills, with very little hail predicted over the boreal forest and coastal plains of northern Manitoba. The local maximum over the foothills of Alberta can be attributed to the mountain–plain circulation frequently advecting moisture from the plains over the foothills. The pooling of moisture in the boundary layer, combined with daytime heating, acts to increase the instability, which results in the formation of thunderstorms over the foothills. This distribution of hail occurrence in Fig. 6a is very similar to that shown in hail climatologies compiled for Canada. For example, Etkin and Brun (1999) estimated the annual number of hail days from synoptic data and found a local maximum of more than 5 hail days per annum over the foothills of southwestern Alberta, with secondary maxima evident over the Peace country over northwestern Alberta and over far southern Saskatchewan

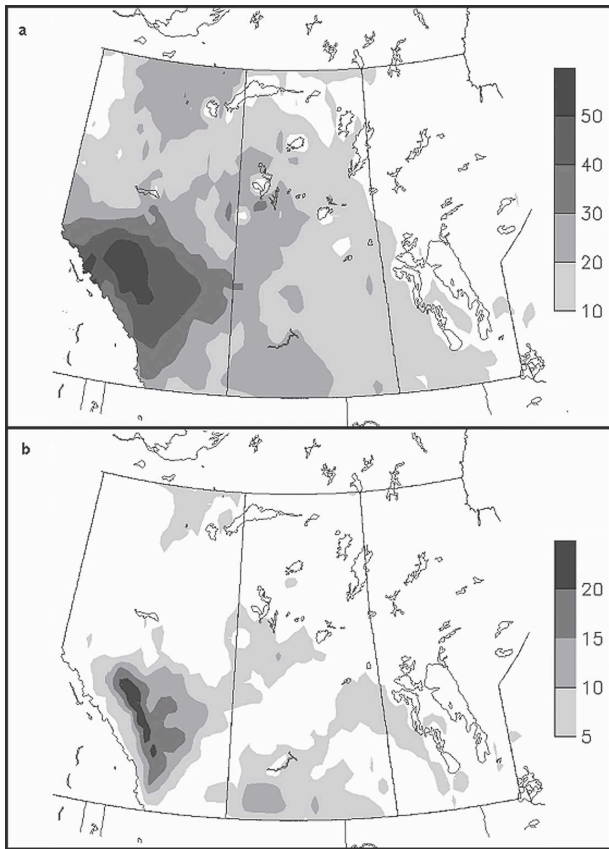


FIG. 6. Accumulated number of forecasted (a) hail days and (b) severe hail days at each GEM model grid point over the Canadian prairie provinces between 1 Jun and 31 Aug 2000.

and Manitoba. Also of note in Fig. 6a are the local minima in forecast hail activity evident above the cooler boundary layer of the large lakes in Manitoba and Saskatchewan, as well as the local maximum over the interlakes region in southern Manitoba.

According to Fig. 6b, more than 20 severe hail days were forecast in a narrow band running parallel to the foothills of southwestern Alberta. This area where a high frequency of severe hail was forecast was very similar to the location of the “hail alley” identified during the Alberta Hail Project (Wojtiw 1977). As was the case for hail days, the number of severe hail days decreased rapidly east of the foothills. A secondary maximum was forecast over southwestern Saskatchewan, which is supported by the local maximum (not shown) of observed severe hail days in that area. Thus, the accumulated hail maps suggest that hail forecasts produced for the Canadian prairie provinces (using the prognostic GEM model soundings) for the summer of 2000 were consistent with the known hail climatology for this region.

8. Conclusions

The objective of this paper was to determine the feasibility of producing spatial maps of the forecast maximum hail size over the Canadian prairie provinces using prognostic GEM model soundings as input for the HAILCAST model. Specifically, the hail forecasts were based on 12-h forecast soundings valid for 0000 UTC each day between 1 June and 31 August 2000. The forecasts of maximum hail size were verified against radar reflectivity data and 533 surface reports of maximum hail size. The verification of the forecasts was focused over the Alberta study area (ASA), a region of about 48 000 km² located in south-central Alberta.

This study has revealed that it is feasible to use prognostic GEM soundings as input data for HAILCAST, making this technique ideal for use in an operational setting. The comparison between radar-derived VIL data and HAILCAST forecasts showed the following:

- 1) HAILCAST is skillful in identifying a hail day versus a nonhail day over the ASA up to 12 h in advance.
- 2) HAILCAST shows skill at distinguishing between severe and nonsevere hail events.
- 3) HAILCAST has limited skill in predicting the distribution of hail on spatial scales less than approximately 60 km, but is skillful at predicting the main threat areas.
- 4) HAILCAST is skillful in predicting the maximum hail diameter.
- 5) Synoptic-scale constraints (such as the presence of a 500-mb trough) are needed to establish whether it is appropriate to run HAILCAST on a given day over Alberta.

Work is under way to correctly identify which GEM model field is most appropriate to identify in advance whether there will be deep convection and at which model grid points HAILCAST should be run. We also plan to determine whether information from the ensemble runs could offer further insight to forecasters. For example, a probabilistic approach may assist in predicting the location and size of hail, with maps showing the probability of hail diameter exceeding certain thresholds, as well as the standard deviation of the forecast hail sizes. This in turn could be useful for generating public forecasts of the probability of hail, a technique that is not currently done in Canada. There are potentially significant economic gains to be realized by any method that can improve the accuracy of public forecasts of severe hail. For example, farmers can move equipment and small livestock indoors, aircraft at aerodromes can be moved indoors, and the public can

move cars and other valuable items located outdoors under cover.

Acknowledgments. This research was supported by grants from the Canadian Foundation for Climate and Atmospheric Sciences (CFCAS), the Natural Sciences and Engineering Research Council (NSERC), and Environment Canada. The authors wish to express their gratitude to the following individuals and organizations for their assistance in undertaking this research: Brad Shannon, Gary Burke, Neil Taylor, Patrick McCarthy, the Alberta Severe Weather Management Society, and the Alberta Agriculture Financial Services Corporation.

REFERENCES

- Baldwin, M. E., J. S. Kain, and M. P. Kay, 2002: Properties of the convection scheme in NCEP's Eta Model that affect forecast sounding interpretation. *Wea. Forecasting*, **17**, 1063–1079.
- Barge, B. L., 1974: Polarization measurements of precipitation backscatter in Alberta. *J. Rech. Atmos.*, **8**, 163–173.
- Betts, A. K., 1986: A new convective adjustment scheme. Part I: Observational and theoretical basis. *Quart. J. Roy. Meteor. Soc.*, **112**, 677–692.
- , and M. J. Miller, 1986: A new convective adjustment scheme. Part II: Single column tests using GATE wave, BOMEX, ATEX and arctic air-mass data sets. *Quart. J. Roy. Meteor. Soc.*, **112**, 693–709.
- Brimelow, J. C., 1999: Numerical modelling of hailstone growth in Alberta storms. M.S. thesis, Dept. of Earth and Atmospheric Sciences, University of Alberta, 153 pp.
- , T. W. Krauss, and G. W. Reuter, 2002a: Operational forecasts of maximum hailstone diameter in Mendoza, Argentina. *J. Wea. Mod.*, **34**, 8–17.
- , G. W. Reuter, and E. P. Poolman, 2002b: Modeling maximum hail size in Alberta thunderstorms. *Wea. Forecasting*, **17**, 1048–1062.
- , —, A. Bellon, and D. Hudak, 2004: A radar-based methodology for preparing a severe thunderstorm climatology in central Alberta. *Atmos.–Ocean*, **42**, 13–22.
- Brooks, H. E., C. A. Doswell III, and R. A. Maddox, 1992: On the use of mesoscale and cloud-scale models in operational forecasting. *Wea. Forecasting*, **7**, 120–132.
- , —, and J. Cooper, 1994: On the environments of tornadic and nontornadic mesocyclones. *Wea. Forecasting*, **9**, 606–618.
- Case, J. L., J. Manobianco, A. V. Dianic, M. M. Wheeler, D. E. Harms, and C. R. Parks, 2002: Verification of high-resolution RAMS forecasts over east-central Florida during the 1999 and 2000 summer months. *Wea. Forecasting*, **17**, 1133–1151.
- Changnon, S. A., 1992: Temporal and spatial relations between hail and lightning. *J. Appl. Meteor.*, **31**, 587–604.
- , R. A. Pielke Jr., D. Changnon, R. T. Sylvés, and R. Pulwarty, 2000: Human factors explain the increased losses from weather and climate extremes. *Bull. Amer. Meteor. Soc.*, **81**, 437–442.
- Charlton, R. B., B. M. Kachman, and L. Wojtiw, 1995: Urban hailstorms: A view from Alberta. *Nat. Hazards*, **12**, 29–75.
- Côté, J., S. Gravel, A. Méthot, A. Patoine, M. Roch, and A. Staniforth, 1998: The operational CMC-MRB Global Environmental Multiscale (GEM) model. Part I: Design considerations and formulation. *Mon. Wea. Rev.*, **126**, 1373–1395.
- Crook, N. A., 1996: Sensitivity of moist convection forced by boundary layer processes to low-level thermodynamic fields. *Mon. Wea. Rev.*, **124**, 1767–1785.
- Dixon, M., and G. Wiener, 1993: TITAN: Thunderstorm Identification, Tracking, Analysis, and Nowcasting—A radar-based methodology. *J. Atmos. Oceanic Technol.*, **10**, 785–797.
- Doswell, C. A., III, J. T. Schaefer, D. W. McCann, T. W. Schlatter, and H. B. Wobus, 1982: Thermodynamic analysis procedures at the National Severe Storms Forecast Center. Preprints, *Ninth Conf. Weather Forecasting and Analysis*, Seattle, WA, Amer. Meteor. Soc., 304–309.
- Edwards, R., and R. L. Thompson, 1998: Nationwide comparisons of hail size with WSR-88D vertically integrated liquid water and derived thermodynamic sounding data. *Wea. Forecasting*, **13**, 277–285.
- Etkin, D., and S. E. Brun, 1999: A note on Canada's hail climatology: 1977–1993. *Int. J. Climatol.*, **19**, 1357–1373.
- Foster, D. S., and F. C. Bates, 1956: A hail size forecasting technique. *Bull. Amer. Meteor. Soc.*, **37**, 135–140.
- Fritsch, J. M., and C. F. Chappell, 1980: Numerical prediction of convectively driven mesoscale pressure systems. Part I: Convective parameterization. *J. Atmos. Sci.*, **37**, 1722–1733.
- , and J. Kain, 1993: Convective parameterization for mesoscale models: The Fritsch–Chappell scheme. *The Representation of Cumulus Convection in Numerical Models*, Meteor. Monogr., No. 46, Amer. Meteor. Soc., 159–164.
- Grell, G. A., 1993: Prognostic evaluation of assumptions used by cumulus parameterizations. *Mon. Wea. Rev.*, **121**, 764–787.
- , Y. Kuo, and R. J. Pasch, 1991: Semiprognostic tests of cumulus parameterization schemes in the middle latitudes. *Mon. Wea. Rev.*, **119**, 5–31.
- Hamill, T. M., and A. T. Church, 2000: Conditional probabilities of significant tornadoes from RUC-2 forecasts. *Wea. Forecasting*, **15**, 461–475.
- Hanna, S. R., and R. Yang, 2001: Evaluations of mesoscale models' simulations of near-surface winds, temperature gradients, and mixing depths. *J. Appl. Meteor.*, **40**, 1095–1104.
- Hart, R. E., G. S. Forbes, and R. H. Grumm, 1998: The use of hourly model-generated soundings to forecast mesoscale phenomena. Part I: Initial assessment in forecasting warm-season phenomena. *Wea. Forecasting*, **13**, 1165–1185.
- Janjić, Z. I., 1994: The step-mountain eta coordinate model: Further developments of the convection, viscous sublayer, and turbulence closure schemes. *Mon. Wea. Rev.*, **122**, 927–945.
- Jewell, R., and J. C. Brimelow, 2004: Evaluation of an Alberta hail growth model using severe hail proximity soundings in the United States. Preprints, *22d Conf. on Severe Local Storms*, Hyannis, MA, Amer. Meteor. Soc., CD-ROM, P9.5.
- Joe, P., D. Burgess, R. Potts, T. Keenan, G. Stumpf, and A. Treloar, 2004: The S2K severe weather detection algorithms and their performance. *Wea. Forecasting*, **19**, 43–63.
- Kitzmler, D. H., W. E. McGovern, and R. F. Saffle, 1995: The WSR-88D severe weather potential algorithm. *Wea. Forecasting*, **10**, 141–159.
- Lenning, E., H. E. Fuelberg, and A. I. Watson, 1998: An evaluation of WSR-88D severe hail algorithms along the northeastern Gulf coast. *Wea. Forecasting*, **13**, 1029–1045.
- Marzban, C., and G. J. Stumpf, 1998: A neural network for damaging wind prediction. *Wea. Forecasting*, **13**, 151–163.
- , and A. Witt, 2001: A Bayesian neural network for severe-hail size prediction. *Wea. Forecasting*, **16**, 600–610.

- Moore, J. T., and J. P. Pino, 1990: An interactive method for estimating maximum hailstone size from forecast soundings. *Wea. Forecasting*, **5**, 508–526.
- Mueller, C. K., J. W. Wilson, and N. A. Crook, 1993: The utility of sounding and mesonet data to nowcast thunderstorm initiation. *Wea. Forecasting*, **8**, 132–146.
- Paxton, C. H., and J. M. Shepherd, 1993: Radar diagnostic parameters as indicators of severe thunderstorms in central Florida. NOAA Tech. Memo. NWS-SR 149, 12 pp. [Available from NTIS, U.S. Department of Commerce, 5285 Port Royal Rd., Springfield, VA 22161.]
- Renick, J. H., and J. B. Maxwell, 1977: Forecasting hailfall in Alberta. *Hail: A Review of Hail Science and Hail Suppression, Meteor. Monogr.*, No. 38, Amer. Meteor. Soc., 145–151.
- Smith, S. B., and M. K. Yau, 1993: The causes of severe convective outbreaks in Alberta. Part II: Conceptual model and statistical analysis. *Mon. Wea. Rev.*, **121**, 1126–1134.
- Stensrud, D. J., J.-W. Bao, and T. T. Warner, 2000: Using initial condition and model physics perturbations in short-range ensembles of mesoscale convective systems. *Mon. Wea. Rev.*, **128**, 2077–2107.
- Thompson, R. L., 1998: Eta Model storm-relative winds associated with tornadic and nontornadic supercells. *Wea. Forecasting*, **13**, 125–137.
- , R. Edwards, J. A. Hart, K. L. Elmore, and P. Markowski, 2003: Close proximity soundings within supercell environments obtained from the Rapid Update Cycle. *Wea. Forecasting*, **18**, 1243–1261.
- Wagenmaker, R. B., 1992: Operational detection of hail by radar using heights of VIP-5 reflectivity echoes. *Natl. Wea. Dig.*, **17**(2), 2–5.
- Weckwerth, T. M., 2000: The effect of small-scale moisture variability on thunderstorm initiation. *Mon. Wea. Rev.*, **128**, 4017–4030.
- Weiss, S. J., D. L. Kelly, and J. T. Schaefer, 1980: New objective verification techniques at the National Severe Storms Forecast Center. Preprints, *Eighth Conf. on Weather Forecasting and Analysis*, Denver, CO, Amer. Meteor. Soc., 412–419.
- Witt, A., M. D. Eilts, G. J. Stumpf, J. T. Johnson, E. D. Mitchell, and K. W. Thomas, 1998: An enhanced hail detection algorithm for the WSR-88D. *Wea. Forecasting*, **13**, 286–303.
- Wojtiw, L., 1977: Climatology of hailstorms in central Alberta. *Albertan Geogr.*, **13**, 15–30.